

Transition from isolated to overlapping resonances in the open system of interacting fermions

G.L. Celardo,¹ F.M. Izrailev,¹ V.G. Zelevinsky,² and G.P. Berman³

¹*Instituto de Física, Universidad Autónoma de Puebla,
Apartado Postal J-48, Puebla, Pue., 72570, México*

²*NSCL and Department of Physics and Astronomy,
Michigan State University, East Lansing, Michigan 48824-1321, USA.*

³*Theoretical Division and CNLS, Los Alamos National Laboratory, Los Alamos, New Mexico 87545, USA.*

(Dated: December 2, 2024)

We study the statistical properties of resonance widths and spacings in an open system of interacting fermions. At the transition between isolated and overlapping resonances, a radical change in the width distribution occurs with segregation of broad (“super-radiant”) and narrow (“trapped”) states. Our main interest is to reveal how this transition is influenced by the onset of chaos in the internal dynamics regulated by the strength of random two-body interaction. In the transitional region, the width distribution and its variance, as well as the distribution of spacings between resonances are strongly affected by internal chaos. The results may be applied to the analysis of neutron cross sections, as well as in the physics of mesoscopic devices with strongly interacting electrons.

PACS numbers: 05.50.+q, 75.10.Hk, 75.10.Pq

Physics of marginally stable mesoscopic systems is an important part of current scientific interest, both in nuclear physics and in condensed matter physics. The center of attention in nuclear physics moved to nuclei far from the valley of stability. Exotic nuclei have low binding energy so that the continuum states are easily excited by a weak external perturbation and appear as the closest virtual states in quantum-mechanical calculations. The correct description of interplay between reactions and intrinsic structure is also important for practical applications connected to neutron cross sections at low and intermediate energy. Mesoscopic solid-state devices, such as quantum dots and quantum wires, are open being explicitly coupled to the outside world. In all such cases, a transition from a consideration of a closed model system to a realistic open system in its interaction with continuum becomes necessary.

A working instrument in the unified description of intrinsic states and reactions, or decay channels, is an *effective non-Hermitian Hamiltonian* \mathcal{H} derived by elimination of channel variables, for example with the help of the projection method [1, 2, 3, 4, 5]. This Hamiltonian describes the intrinsic dynamics of an open system; its eigenvalues are *complex energies*, $\mathcal{E}_j = E_j - \frac{i}{2}\Gamma_j$, where the width Γ determines the lifetime of the resonance, $\tau \sim \hbar/\Gamma$. The imaginary part of \mathcal{H} , factorized in the amplitudes of entrance and exit channels, is dictated by the unitarity of the scattering matrix. The factorization brings in remarkable consequences observed in numerical simulations [6] and explained theoretically in Refs. [7], where the analogy to optical *superradiance* [8] of coherently radiating atomic emitters was pointed out. When typical widths Γ are small compared to the level spacing, D , on the real energy axis, $\Gamma/D \ll 1$, the cross sections display *isolated* resonances. In the critical region $\Gamma/D \approx 1$ with crossover to *overlapping* resonances, the width distribution displays sharp segregation of broad

short-lived (*superradiant*) states and very narrow long-lived (*trapped*) states [4, 7, 9]. Correspondingly, the distribution of poles of the scattering matrix undergoes a sharp transition from one to two “clouds” of poles in the complex plane of resonance energies [10].

Below we study the statistical properties of resonance widths and spacings in the transitional regime explicitly taking into account the regular or chaotic dynamics inside the system [11, 12]. The local statistical properties of chaotic states can be identified with those of the Gaussian Orthogonal Ensemble (GOE) [13]. Here, for the first time, the truly *two-body random ensemble* (TBRE) for the intrinsic interaction is considered that allows one to vary the degree of internal chaos in an open system. With the non-Hermitian approach, random two-body dynamics was used in Ref. [14] in the limit of a very strong interaction, when the influence of the mean field was neglected.

We consider a set of a large number, N , of intrinsic many-body states $|i\rangle$ with the same exact quantum numbers. The states are unstable being coupled to M open decay channels. The dynamics of the whole system is governed by an effective non-Hermitian Hamiltonian [2, 7] given by a sum of two $N \times N$ matrices,

$$\mathcal{H} = H - \frac{i}{2}W; \quad W_{ij} = \sum_{c=1}^M A_i^c A_j^c; \quad (1)$$

the intrinsic states are labeled as i, j, \dots and decay channels as a, b, c, \dots . Here H describes Hermitian internal dynamics, while W contains the amplitudes A_i^c coupling intrinsic states $|i\rangle$ to the channels c . Under time-reversal invariance, both H and W are real symmetric matrices.

We model H by the TBRE for n fermions distributed over m single-particle states; the total number of many-body states is $N = m!/[n!(m-n)!]$; in our simulations $n = 6$, $m = 12$, $N = 924$. In the TBRE, $H = H_0 + V$,

where H_0 describes the mean field part, where single-particle energies, ϵ_s , are assumed to have a Poissonian distribution of spacings, with the mean level density $1/d_0$. The two-body interaction V between the particles [12] is fixed by the variance of the two-body random matrix elements, $\langle V_{s_1,s_2;s_3,s_4}^2 \rangle = v_0^2$. While at $v_0 = 0$ we have a Poissonian spacing distribution $P(s)$ of many-body states, for $d_0 = 0$ (infinitely strong interaction, $v_0 \rightarrow \infty$), $P(s)$ is close to the Wigner-Dyson (WD) distribution typical for a chaotic system. The critical interaction for the onset of strong chaos is given [12] by $v_{cr}/d_0 \approx 2(m-n)/N_s$, where $N_s = n(m-n)[1+(n-1)(m-n-1)/4]$ is the number of directly coupled many-body states in any row of the matrix H_{ij} . Thus, we have $v_{cr}/d_0 \approx 1/20$, and often we have used the value $v_0/d_0 = 1/30$ slightly less than v_{cr} . In parallel we also consider H as a member of the GOE [7, 15] that corresponds to a *many-body* interaction, when the matrix elements are Gaussian random variables, $\langle H_{ij}^2 \rangle = 1/N$ for $i \neq j$ and $\langle H_{ij}^2 \rangle = 2/N$ for $i = j$.

The real amplitudes A_i^c are assumed to be random independent Gaussian variables with zero mean and correlator $\langle A_i^c A_j^{c'} \rangle = \delta_{ij} \delta^{cc'} \gamma^c / N$. This is compatible with the GOE or TBRE assumed for intrinsic dynamics when generic many-body states coupled to continuum have complicated structure, while the decay probes specific simple components of these states related to few open channels. The parameters γ^c with dimension of energy characterize the coupling to the channel c . Such a normalization is convenient if the energy interval ND covered by decaying states is finite. We neglect a possible explicit energy dependence of amplitudes (the transitional region is far from thresholds).

The effective Hamiltonian (1) determines the reaction cross sections, $\sigma^{ba}(E) \propto |T^{ba}(E)|^2$, or the scattering matrix $S = 1 - iT$. The reaction amplitudes, neglecting the smooth potential phases irrelevant for our purposes, are expressed in terms of the amplitudes A_i^c :

$$T^{ba}(E) = \sum_{i,j}^N A_i^b \left(\frac{1}{E - \mathcal{H}} \right)_{ij} A_j^a. \quad (2)$$

The complex eigenvalues \mathcal{E}_j of \mathcal{H} coincide with the poles of the S -matrix and, for small γ^c , determine energies and widths of separated resonances. In the simulations we consider an energy interval at the center of the spectrum of \mathcal{H} with the constant level density $\rho(0) = D^{-1}$. As γ^c grows, the resonances start to overlap, the effective parameter being $\kappa^a = \pi \gamma^a / 2ND$. The transmission coefficient $T^a = 1 - |\langle S^{aa} \rangle|^2$ in the channel a is maximal (equal to 1) at the critical point, $\kappa^a = 1$, that marks the transition to superradiance and trapping. We study the statistical properties of resonance widths and spacings as a function of the interaction between particles (ratio v_0/d_0) and the continuum coupling parameter κ . We assume M equiprobable channels, $\kappa^a = \kappa$; the maximum value of M we considered is $M = 10$. For each value of κ we have used $N_r = 100$ realizations of the Hamiltonian

matrices, with further averaging over energy.

At a critical value $\kappa \approx 1$, a segregation of the resonance widths occurs [6, 7, 10], see inset in Fig. 1. The widths of M resonances are increasing at the expense of the remaining $N - M$ resonances. For weak coupling, $\kappa \ll 1$, the widths are given by diagonal matrix elements, $\Gamma_i = \langle i|W|i \rangle = \sum_{c=1}^M (A_i^c)^2$, and the mean width is $\langle \Gamma \rangle = \gamma M / N$. In the limit of strong coupling, $\kappa \gg 1$, the widths of M broad resonances converge to the non-zero eigenvalues of the matrix W . As for the remaining “trapped” states, their widths decrease $\propto 1/\gamma$.

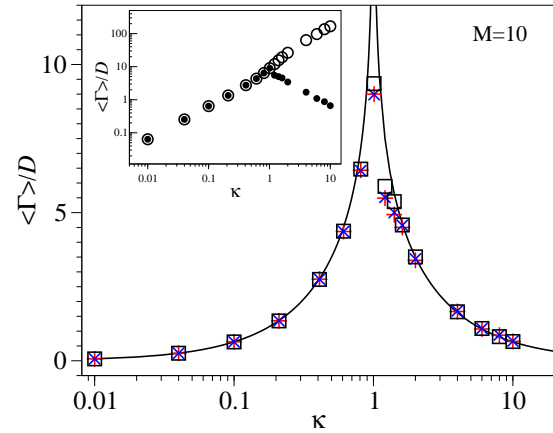


FIG. 1: (Color online) Average width versus the coupling strength κ for $M = 10$. Solid curves show the expression (4), pluses refer to $v_0 = 0$, crosses to $v_0 = d_0/30$, squares to $v_0/d_0 = \infty$. In all cases for $\kappa > 1$ the average was made over $N - M$ narrow resonances only. More details are shown for $v_0 = d_0/30$ in the inset, where open circles correspond to the average over *all* N resonances, and full circles stand for the average over all resonances for $\kappa < 1$, and over $N - M$ narrow resonances for $\kappa > 1$.

In Fig. 1 we show how the average width (normalized to the mean level spacing D) depends on κ for different values of v_0/d_0 . The inset demonstrates a sharp change in the width distribution at the transition point $\kappa = 1$. The results have been compared with the Moldauer-Simonius (MS) relation [16, 17] (that follows also from our statistical assumptions)

$$\sum_{c=1}^M \ln(1 - T^c) = -2\pi \frac{\langle \Gamma \rangle}{D}. \quad (3)$$

For our case of M equivalent channels,

$$\frac{\langle \Gamma \rangle}{D} = \frac{M}{\pi} \ln \left| \frac{1 + \kappa}{1 - \kappa} \right|. \quad (4)$$

Here we put the absolute value of the ratio under the logarithm in order to extrapolate this expression beyond the transition point, for $\kappa > 1$. The extrapolated MS-formula works well for any interaction strength. For one

channel, this result was obtained in Ref. [7, 9]; here we see that the MS-expression is also valid for a large number of channels, independently of the interaction strength. According to [18], the divergence of $\langle \Gamma \rangle$ at $\kappa = 1$ is due to the (non-integrable) power-law behavior for large Γ , see below; in the numerical simulation, see Fig. 1, there is no divergence because of the finite number of resonances.

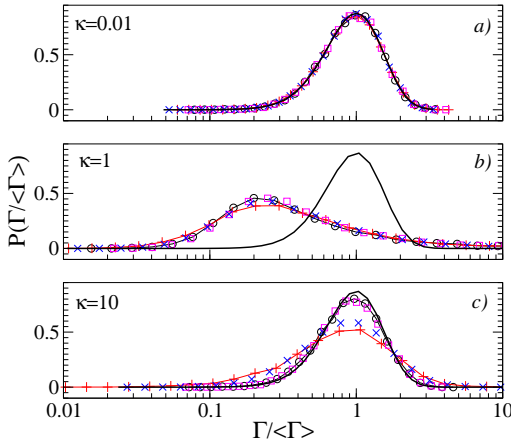


FIG. 2: (Color online) Width distribution for $M = 10$ and $\kappa = 0.01, 1, 10$, with the same symbols as in Fig. 1. Smooth curves are the χ_{10}^2 distribution.

The width distribution $P(\Gamma)$ is shown in Fig. 2 for different values of v_0/d_0 and $\kappa = 0.01, 1, 10$. At weak coupling, Fig. 2a, the conventional χ^2 -distribution is valid for any strength of the interaction. However, when κ increases, Fig. 2b and 2c, a clear dependence on the interaction strength emerges. As first noted in Ref. [19], as κ increases, $P(\Gamma)$ becomes broader than the χ^2 distribution. For large κ , both for the GOE and for $v_0/d_0 \rightarrow \infty$, $P(\Gamma)$ is again given by the χ_M^2 distribution, contrary to the cases of the finite interaction strength; this reflects the uniformity of properties of all fully chaotic intrinsic states.

Apart from the one-channel case studied in Ref. [20], a general analytical treatment of the width distribution is a difficult task even for simplified random matrix models. In the case of GOE for the Hermitian part H_{ij} , the width distribution was found in Ref. [18], neglecting the emergence of broad resonances in the regime of strong overlap at $\kappa > 1$. Our results for $v_0/d_0 = \infty$ correspond well to the analytical predictions. In particular, the tails of $P(\Gamma)$ decrease $\sim \Gamma^{-2}$ that leads to the divergence of $\langle \Gamma \rangle$ in agreement with the MS-formula.

The (normalized) variance of the resonance widths, see Fig. 3 for $M = 10$ and $\kappa = 0.8$, strongly depends on the interaction between particles. Our results confirm the analytical estimate for the transition to strong chaos that can be associated with the WD-distribution of level spacings. Note, however, that the transition is quite smooth, and even for a relatively strong interaction there is a deviation of the variance from the GOE value. We would like to stress that the level spacing distribution, as the

weakest signature of quantum chaos [11], turns out to be rather insensitive to the transition. Indeed, the data in the inset for $\kappa = 0$ roughly correspond to the WD-distribution, although once the continuum coupling is switched on, the variance of the resonance widths is very different from that predicted by the GOE.

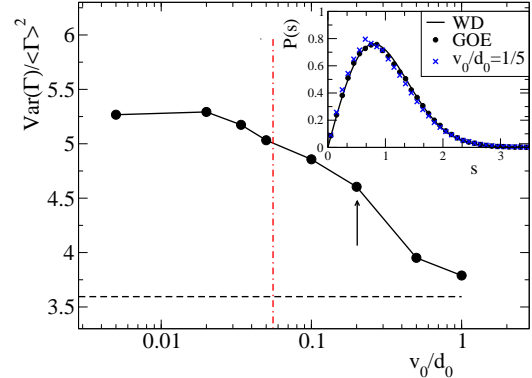


FIG. 3: (Color online) Dimensionless variance of the widths versus v_0/d_0 for $M = 10$ (connected circles): the GOE value is shown by horizontal dashed line; the vertical dot-dashed line marks the value $v_0 = v_{cr}$ corresponding to the onset of chaos. In the inset the level spacing distribution is shown for $v_0/d_0 = 0.2$ (crosses), see the arrow in the main part, and for the GOE (circles). The smooth curve is the WD-distribution.

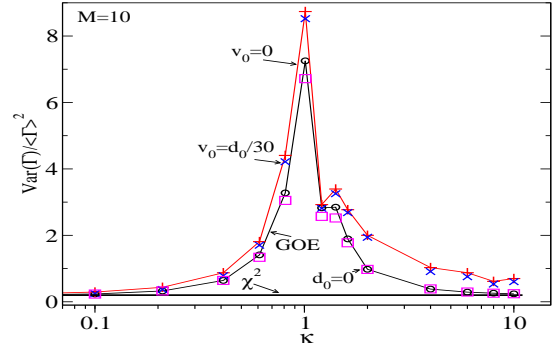


FIG. 4: (Color online) Dimensionless variance of the width vs κ for $M = 10$. The χ_M^2 distribution is shown by the horizontal line; the symbols are the same as in Fig. 1. Non-smooth dependence for $\kappa > 1$ is due to a shift of the critical point for $M \gg 1$ from $\kappa = 1$ to $\kappa = \kappa_c > 1$, see Ref. [10].

It is instructive to show how the variance of the widths depends on the continuum coupling, Fig. 4. The prediction of the χ_M^2 distribution that the variance is $2/M$ independently of κ is correct for very weak and very strong coupling. As expected, the variance takes its maximal value at the transition point $\kappa = 1$ (it diverges for $N \rightarrow \infty$). As for the dependence on v_0 , the less chaotic is the intrinsic dynamics and therefore greater a possible difference in the structure of decaying states, the larger is the width variance. For the GOE and $v_0/d_0 \rightarrow \infty$, the system returns to the χ_M^2 distribution, with an increase

of κ . This is not true for a finite value of v_0/d_0 , in agreement with the results of Ref. [21], where justification of the broadening of the width distribution in the Poisson case (equivalent to $v_0 = 0$) as compared to the GOE was given for $M = 1$.

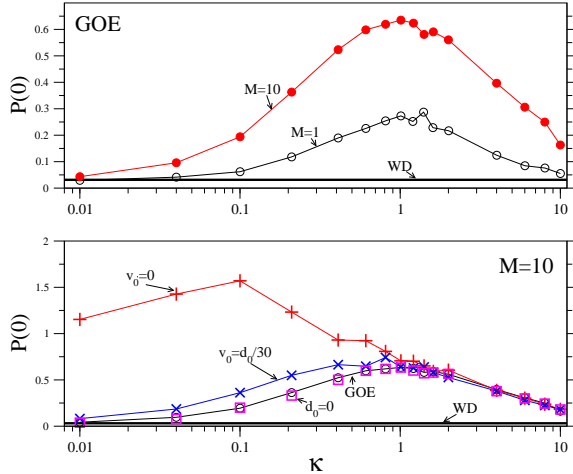


FIG. 5: The probability $P(0)$ of finding the level spacing $s < 0.04$ (in units of mean level spacing) vs κ . Upper panel: GOE for $M = 1$ (open circles) and $M = 10$ (full circles); lower panel: $M = 10$ with the same symbols as in Fig. 1. The value due to the WD-distribution is given by the horizontal line.

Finally, we analyze how the *level repulsion* along the real energy axis depends on the continuum coupling and on the intrinsic interaction. The characteristic quantity is the probability of the level proximity, $P(s \rightarrow 0)$. It is finite for the Poisson distribution and vanishes linearly for the GOE. A weakening of the level repulsion with an increase of the continuum coupling (or the number of channels M) was noted as a generic property in Ref. [19]. The physical explanation (energy uncertainty of quasistationary states) was given in [7]. Our detailed data, Fig. 5, confirm these results and show the dependence on v_0/d_0 . For non-interacting particles, $v_0 = 0$, the results are consistent with those of Ref. [22], where it was argued that, for the Poissonian intrinsic Hamiltonian H , the distribution $P(s)$ becomes similar to that of a chaotic system due to the perturbation induced by the

coupling to the continuum. Our data clearly show that with increase of intrinsic chaos the level repulsion grows, however, for finite v_0 always remains weaker than for the GOE case.

In conclusion, we have studied statistics of complex energies (resonance widths and spacings) for a generic fermion system coupled to open decay channels. For the first time we carefully followed various signatures of the crossover from isolated to overlapping resonances in dependence on the inter-particle interaction. We show that the Moldauer-Simonius expression for average widths is valid also in the region $\kappa > 1$, provided the M widest resonances are excluded. Also, we found that the average widths are insensitive to the interaction strength. On the other hand, the width variance depends on the degree of intrinsic chaos at the transition point $\kappa \approx 1$ in a non-trivial way. Even if for a closed system ($\kappa = 0$) the level spacing distribution is of the Wigner-Dyson form, the width distribution for a perfect coupling to the continuum ($\kappa \approx 1$) is very different from the GOE predictions.

Our study is based on the two-body nature of the inter-particle interaction. However, since we explored the central part of the energy band where the eigenstates are delocalized, one can expect similar statistical properties of resonances if one substitutes the intrinsic interaction V by the GOE matrix, with a proper rescaling of the interacting strength v_0 . This may allow for an accurate analytical analysis. The obtained results can be applied to neutron resonances in nuclei and to open mesoscopic systems in the crossover region, where we found strong deviations from the conventional level statistics and χ^2 width distribution. The results on statistical properties of the reaction cross sections, including Eriscon fluctuations, will be reported elsewhere.

We acknowledge useful discussion with T. Gorin, T. Kawano, D. Savin, and V. Sokolov. The work was supported by the NSF grants PHY-0244453 and PHY-0555366. The work by G.P.B. was carried out under the auspices of the National Nuclear Security Administration of the U.S. Department of Energy at Los Alamos National Laboratory under Contract No. DE-AC52-06NA25396. F.M.I. acknowledges the support by the CONACYT (México) grant No 43730.

[1] H. Feshbach, Ann. Phys. **5**, 357 (1958); **19**, 287 (1962).
[2] C. Mahaux and H.A. Weidenmüller, *Shell Model Approach to Nuclear Reactions* (North Holland, Amsterdam, 1969).
[3] I. Rotter, Rep. Prog. Phys. **54**, 635 (1991).
[4] V.V. Sokolov and V.G. Zelevinsky, Ann. Phys. (N.Y.) **216**, 323 (1992).
[5] A. Volya and V. Zelevinsky, Phys. Rev. Lett. **94**, 052501 (2005); Phys. Rev. C **74**, 064314 (2006).
[6] P. Kleinwächter and I. Rotter, Phys. Rev. C **32**, 1742 (1985).
[7] V. V. Sokolov and V. G. Zelevinsky, Phys. Lett. B **202**, 10 (1988); Nucl. Phys. **A504**, 562 (1989).
[8] R.H. Dicke, Phys. Rev. **93**, 99 (1954).
[9] F.M. Izrailev, D. Sacher and V.V. Sokolov, Phys. Rev. E **49**, 130 (1994).
[10] F. Haake *et al.*, Z.Phys. B **88**, 359 (1992).
[11] V. Zelevinsky, Ann. Rev. Nucl. Part. Sci., **46**, 237 (1996).
[12] V.V. Flambaum and F.M. Izrailev, Phys. Rev. E **56**, 5144 (1997).
[13] T.A. Brody *et al.*, Rev. Mod. Phys. **53**, 385 (1981).
[14] D. Agassi, H.A. Weidenmüller and G. Mantzouranis,

Phys. Rep. **3**, 145 (1975).

- [15] J.J.M. Verbaarschot, H.A. Weidenmüller, and M.R. Zirnbauer, Phys. Rep. **129**, 367 (1985).
- [16] P.A. Moldauer, Phys. Rev. **157**, 907 (1967).
- [17] M. Simonius, Phys. Lett. B **52**, 279 (1974).
- [18] H.-J. Sommers, Y.V. Fyodorov, and M. Titov, J. Phys. A: Math. Gen. **32**, L77 (1999).
- [19] P.A. Moldauer, Phys. Rev. **171**, 1164 (1968).
- [20] S. Mizutori and V.G. Zelevinsky, Z. Phys. **A346**, 1 (1993).
- [21] T. Gorin et al., Phys. Rev. E **56**, 2461 (1997).
- [22] F.M. Dittes, I. Rotter and T.H. Seligman, Phys. Lett. A, **158**, 14 (1991).